AD-A233 098

DOCUMENTATION PAGE

Form Approved
OMB No. 0704-0188

1a. SECURITY CLASSIFICATION AUTHORITY

1b. RESTRICTIVE MARKINGS

2b. DECLASSIFICATION / DOWNGRADING SCHEDULE

3. DISTRIBUTION / AVAILABILITY OF REPORT
Approved for public release; distribution unlimited

4. PERFORMING ORGANIZATION REPORT NUMBER(S)
P90-021

5. MONITORING ORGANIZATION REPORT NUMBER(S)
P90-021

6a. NAME OF PERFORMING ORGANIZATION
U.S. Army Medical Research Institute of Chemical Defense

6b. OFFICE SYMBOL (If applicable)
SGRD-UV-YN

7a. NAME OF MONITORING ORGANIZATION
U.S. Army Medical Research Institute of Chemical Defense, SGRD-UV-RC

6c. ADDRESS (City, State, and ZIP Code)
Aberdeen Proving Ground, Md 21010-5425

7b. ADDRESS (City, State, and ZIP Code)
Aberdeen Proving Ground, MD 21010-5425

8a. NAME OF FUNDING / SPONSORING ORGANIZATION

8b. OFFICE SYMBOL (If applicable)

9. PROCUREMENT INSTRUMENT IDENTIFICATION NUMBER

8c. ADDRESS (City, State, and ZIP Code)

10. SOURCE OF FUNDING NUMBERS

PROGRAM ELEMENT NO.	PROJECT NO.	TASK NO.	WORK UNIT ACCESSION NO.
61102A	3M161102B	S11 AA	

11. TITLE (Include Security Classification)
Effects of Pentobarbital on Respiratory Functional Dynamics in Chronically Instrumented Guinea Pigs

12. PERSONAL AUTHOR(S)

13a. TYPE OF REPORT	13b. TIME COVERED	14. DATE OF REPORT (Year, Month, Day)	15. PAGE COUNT
Open Literature Publ	FROM _____ TO _____		10

16. SUPPLEMENTARY NOTATION
Brain Research Bulletin, Vol. 26, pp123-132

17. COSATI CODES		
FIELD	GROUP	SUB-GROUP
06	15	
06	04	

18. SUBJECT TERMS (Continue on reverse if necessary and identify by block number)
sodium pentobarbital; respiration; chronic single unit recording; diaphragmatic EMG; guinea pigs

19. ABSTRACT (Continue on reverse if necessary and identify by block number)

CHANG, F.-C. T. *Effects of pentobarbital on respiratory functional dynamics in chronically instrumented guinea pigs.* BRAIN RES BULL 26(1) 123–132, 1991.—Respiratory effects of sodium pentobarbital (35 mg/kg; IP) were studied in guinea pigs chronically instrumented to permit concurrent recordings of bulbar respiratory-related units (RRUs), diaphragmatic electromyogram (DEMG), and electrocorticogram (ECoG). RRU activities were recorded from either the Bötzinger Complex (BOT; expiratory) or Nucleus para-Ambiguus (NpA; inspiratory). Pentobarbital-induced changes in respiratory-related activities were evaluated before, throughout the course of, and during recovery from, anesthesia. The most notable development following pentobarbital was a state of progressive bradypnea which was accompanied by a variety of complex changes in the amplitude and temporal attributes of RRU, DEMG and ECoG activities. As anesthetic effects progressed, the activity profiles of both BOT and NpA units underwent striking transformations from a behavioral and state-dependent wakefulness pattern to an activity profile characterized by i) a significantly augmented RRU cycle duration, burst duration and spike frequency; and, ii) an alteration to the pattern of within-burst spike frequency modulation. Along with changes in RRU activity, pentobarbital also produced a marked attenuation of the amplitudes of diaphragmatic activity as well as a discrete, time-dependent alteration in the amplitude and spectral characters of ECoG activities. Differences in BOT and NpA unit responses to alveolar CO_2 loading (ramp; 2% and 5%) across wakefulness and anesthesia states were also considerable. In addition to a depressed responsiveness to CO_2, the temporal attributes of BOT and NpA activity profiles also indicated an asymmetrical change under pentobarbital anesthesia. Taken together, these findings indicate that pentobarbital causes not only a fundamental alteration in bulbar rhythmogenic mechanisms, but also a differential influence on bulbar respiratory system compo-

20. DISTRIBUTION / AVAILABILITY OF ABSTRACT
☐ UNCLASSIFIED/UNLIMITED ☒ SAME AS RPT. ☐ DTIC USERS

21. ABSTRACT SECURITY CLASSIFICATION

22a. NAME OF RESPONSIBLE INDIVIDUAL	22b. TELEPHONE (Include Area Code)	22c. OFFICE SYMBOL
Baze, Wallace B., LTC, VC	301-671-2553	SGRD-UV-YN

DD Form 1473, JUN 86 *Previous editions are obsolete.* SECURITY CLASSIFICATION OF THIS PAGE

17. cont'd

06 11

19. Cont'd

nents that are involved in the definition of the shape and the amplitude of central respiratory drive. In conclusion, this study offers, for the first time, direct evidence from physiologically and structurally intact preparations that the functional dynamics of respiratory system components are profoundly altered during pentobarbital anesthesia.

Brain Research Bulletin, Vol. 26, pp. 123–132. Pergamon Press plc, 1991. Printed in the U.S.A. 0361-9230/91 $3.00 + .00

Effects of Pentobarbital on Respiratory Functional Dynamics in Chronically Instrumented Guinea Pigs

FAT-CHUN T. CHANG

Neurotoxicology Branch, Pathophysiology Division
U.S. Army Medical Research Institute of Chemical Defense, Aberdeen Proving Ground, MD 21010-5425

Received 21 May 1990

CHANG, F.-C. T. *Effects of pentobarbital on respiratory functional dynamics in chronically instrumented guinea pigs.* BRAIN RES BULL **26**(1) 123–132, 1991.—Respiratory effects of sodium pentobarbital (35 mg/kg; IP) were studied in guinea pigs chronically instrumented to permit concurrent recordings of bulbar respiratory-related units (RRUs), diaphragmatic electromyogram (DEMG), and electrocorticogram (ECoG). RRU activities were recorded from either the Bötzinger Complex (BOT; expiratory) or Nucleus para-Ambiguus (NpA; inspiratory). Pentobarbital-induced changes in respiratory-related activities were evaluated before, throughout the course of, and during recovery from, anesthesia. The most notable development following pentobarbital was a state of progressive bradypnea which was accompanied by a variety of complex changes in the amplitude and temporal attributes of RRU, DEMG and ECoG activities. As anesthetic effects progressed, the activity profiles of both BOT and NpA units underwent striking transformations from a behavioral and state-dependent wakefulness pattern to an activity profile characterized by i) a significantly augmented RRU cycle duration, burst duration and spike frequency; and, ii) an alteration to the pattern of within-burst spike frequency modulation. Along with changes in RRU activity, pentobarbital also produced a marked attenuation of the amplitudes of diaphragmatic activity as well as a discrete, time-dependent alteration in the amplitude and spectral characters of ECoG activities. Differences in BOT and NpA unit responses to alveolar CO_2 loading (ramp; 2% and 5%) across wakefulness and anesthesia states were also considerable. In addition to a depressed responsiveness to CO_2, the temporal attributes of BOT and NpA activity profiles also indicated an asymmetrical change under pentobarbital anesthesia. Taken together, these findings indicate that pentobarbital causes not only a fundamental alteration in bulbar rhythmogenic mechanisms, but also a differential influence on bulbar respiratory system components that are involved in the definition of the shape and the amplitude of central respiratory drive. In conclusion, this study offers, for the first time, direct evidence from physiologically and structurally intact preparations that the functional dynamics of respiratory system components are profoundly altered during pentobarbital anesthesia.

Sodium pentobarbital Respiration Chronic single unit recording Diaphragmatic EMG Guinea pigs

PENTOBARBITAL has been shown to exert profound influences over a wide range of respiratory-related activities. These include a blunted Breuer-Hering reflex (4, 17, 23), a dose-dependent depression on selected populations of ponto-medullary respiratory neurons (2, 5, 8, 17, 26), a diminished responsiveness to hypercapnia and hypoxia (25,30), and a direct depressant effect on diaphragmatic neurotransmission (27). While these findings have added to our knowledge and heightened our awareness about the aberrant effects of pentobarbital on respiration, the experimental approaches employed in these investigations remained, however, somewhat questionable. More specifically, in studies that attempted to investigate the central effects of pentobarbital, the functional and structural integrities of experimental animals were invariably reduced or modified to a varying degree with such procedures as vagotomy, decerebration, neuromuscular paralysis, and/or corruption with a preexisting local and/or general anesthetic agent (1, 2, 5, 8, 16, 18, 25, 26, 30). Thus, even if the information derived from such preparations could shed some light on where and how pentobarbital acts to produce its effects, we would still be faced with the quandary that the findings are not truly representative of the "normal" state. In studies where conscious animals were used [e.g., (4, 7, 23)], the effects of pentobarbital on central respiratory rhythmogenic mechanisms were neither adequately identified nor directly measured.

The purpose of this study was to conduct an electrophysiological survey of pentobarbital's effects on bulbar and diaphragmatic respiratory system components in a freely behaving, functionally and structurally intact animal model system: A methodological alternative which was not previously available to respiratory neurobiologists. When instrumented, this model permits concurrent recordings of single medullary respiratory-related unit (RRU) activity, diaphragmatic electromyogram (DEMG) and electrocorticogram (ECoG). This model system together with findings reported here may serve to initiate more systematic approaches in identifying and characterizing the sites and mechanisms through which anesthetic agents exert their respiratory depressant effects.

Two medullary respiratory-related areas were selected as the focus of this study. These are the Bötzinger Complex [BOT; (20–22)] and the Nucleus para-Ambiguus [NpA; (19)]. The majority of BOT neurons display an expiratory activity pattern and they have been shown to exert powerful inhibition and modulatory influences over the entire medullary inspiratory neurons as well

as the spinal phrenic nuclei (3, 13, 20). Functionally, BOT neurons play an important role not only in the definition of the rate, the shape, and the depth of respiratory drive, but also in the maintenance of synchronized respiratory activities of the hemimedullae. Respiratory-related neurons in NpA are primarily of the inspiratory type and are involved in the final stage of bulbar inspiratory motor outflow (6,7).

METHOD

Nineteen male Hartley albino guinea pigs (*Cavia porcellus*), weighing 500–750 g, were used in this study. These animals were housed in plastic cages with ad lib access to food and water. The animal colony was maintained at a constant temperature (22 ± 2°C) with an artificial 12-h light-dark cycle.

Chronic Instrumentation Procedure

All surgical procedures were performed under aseptic conditions. Prior to surgery, an antibiotic (chloramphenicol, 30 mg/kg; IM) was administered 1 day, and 1 h before the induction of surgical anesthesia. Upon completion of surgery, the antibiotic agent was administered once each day for 3 consecutive days. Each animal was initially anesthetized to a surgical level with sodium pentobarbital (38 mg/kg; IP). Corneal reflex and reactions to toe pinching were regularly examined to ensure adequate depth of anesthesia during surgery. Whenever necessary, a supplemental dose of pentobarbital (5 mg/kg; IP) was administered to maintain the surgical level of anesthesia. The core temperature was maintained between 38–39°C with a servo-controlled thermal blanket throughout the course of surgery.

Each animal was chronically instrumented for electrophysiological recordings of medullary RRU activity, DEMG, and ECoG. Readers are referred to previously published reports for more information concerning the chronic DEMG (10) and single unit (11) instrumentation procedures.

Instrumentation for chronic diaphragmatic electromyographic recording [see (10) for details]. DEMG activities were recorded differentially for better signal-to-noise ratio and for common mode rejection of cardiac activity and other unwanted artifacts. DEMG electrodes were made from a pair of Teflon-coated, flexible, multistranded stainless steel wires (Type AS-633 or AS-634, Cooner Wire Co., Chatsworth, CA). Surgical cut-down involved a small incision (10 to 15 mm; on the right side of the body) starting at a point ventral to the tip of the 11th rib and coursing in a rostroventral direction toward the xiphisternum cartilage. The abdominal cavity was then exposed by teasing the muscle layers with blunt surgical tweezers. Access to the right costal diaphragm was accomplished by retracting the liver and other abdominal tissues with blunt surgical instruments. An optical fiber light source was used in visualizing the rhythmically contracting costal diaphragm at the time of electrode insertion. The rostral ends of the electrodes were back-loaded into a 7-cm long, half-circle hypodermic needle (Becton Dickinson, Rutherford, NJ). The sharp tip of the needle was then pushed through the diaphragm, into the pleural cavity, and retrieved after its exit between the eighth and ninth intercostal space. After ensuring sufficient wire length beyond the exit point for handling, the hypodermic needle was removed from the electrode wires. DEMG signals were electrophysiologically verified prior to closing of the wounds. Allowing adequate return tension, the wires were threaded subcutaneously to the head. Longitudinally separated abnominal muscles and the incision were then closed with surgical silk. The final wiring and fashioning of an acrylic head-mound were not made until instrumentations of ECoG and single unit recording electrodes had been completed.

Instrumentation for electrocorticographic (ECoG) recording. Standard surgical instrumentation procedures were followed for chronic ECoG recording. Stainless steel skull screws with Teflon-insulated electrical leads (32 ga) flux-soldered to the screw-head were inplanted bilaterally over the parietal cortices (2 mm caudal to the coronal suture; 1.5 mm medial to the temporal crest) for the differentiation of ECoG signals. A third cortical screw serving as signal ground was placed in the frontal bone midway between the midline and the arched portion of the orbital crest.

Instrumentation for chronic unit recording [see (11) for details]. RRU electrodes (37.5 μm in diameter; Z = 100–500 kΩ at 1 kHz) were constructed from stress-relieved Formvar or Polyamide-insulated platinum (90%)-iridium (10%) finewires (California Finewire Company, Grover City, CA). To enable unit isolation, an implantable microdrive was used. To allow access to lower brainstem neurons, a small hole (approximately 1 mm in diameter) was drilled through the calvarium at a stereotaxically determined point just dorsal to the target area. A small portion of the underlying meninges was carefully teased apart with microsurgical instruments. With the microdrive assembly in its stereotaxic holder, a single-strand finewire was advanced vertically down into the inner guide tube of the microdrive, through the underlying neural tissues, to finally reach the brainstem target area. Neuronal activities were monitored en route with standard extracellular electrophysiological techniques. Once the target neuron of interest had been identified, the tip of the finewire was raised by approximately 100–200 μm to avoid unnecessary damage to the target area during the postoperative recovery period. A small drop of cyanoacrylate adhesive was used to cement the finewire to the upper opening of the inner guide tube. When the adhesive was completely dry, the finewire was carefully liberated from the stereotaxic holder. After the skull hole had been filled with melted bone wax, dental cement was applied to fix the miniature microdrive block to the calvarium. The finewire, animal ground wires, DEMG and ECoG electrodes were all routed to the connector strips rostral to the microdrive assembly. Additional dental cement was applied to finally complete the fashioning of the head mound. Animals were allowed to recover for at least 2 weeks prior to experimentation.

Experimental Procedure

Environment and equipment for chronic electrophysiological recording. Upon recovery from surgery, the guinea pig was placed in, and acclimated to, a noise-attenuated Faraday chamber (30 cm in width and length, 40 cm in height). Aside from the minor restriction imposed by the signal transmission tether, the animal was free to move within the perimeter of the Faraday cage. Respiratory-related unit activities were isolated with the aid of a chronically implanted microdrive (vide supra). Standard extracellular electrophysiological criteria were followed in unit isolation and sampling which included i) invariant temporal characteristics of spike waveform (signature) and spike duration; and ii) stability of signal amplitude. Unit, DEMG and ECoG signals were amplified (Neurolog Model NL104 AC Preamplifier, Digitimer Ltd.) and band-pass filtered (RRU, 300–10,000 Hz; DEMG, 50–7,500 Hz; ECoG, 0.5–500 Hz; Neurolog Model NL 126 passive filter, Digitimer Ltd.). RRU, DEMG and ECoG activities were displayed on an oscilloscope and recorded with a 14-channel FM tape recorder (TEAC XR510WB). Respiratory-related behaviors were documented with an audio-visual recording system which consisted of a video camera (Panasonic WV-6000), a video cassette recorder (Panasonic AG-1800) and a video monitor (Sony CVM-1271). Because each animal served as its own control, a period of 45-min control recording was performed prior to the induction of pentobarbital anesthesia.

Induction of pentobarbital anesthesia. At the conclusion of the control period, the animal was anesthetized with sodium pen-

tobarbital (35 mg/kg; IP). Upon complete loss of the righting reflex, the animal was wrapped in a servo-controlled thermal blanket and its core temperature maintained between 38–39°C.

Response categories. Respiratory responses to pentobarbital were categorized and analyzed on the basis of 3 experimental periods. These were Transitional, Steady-State, and Recovery periods. The periods were operationally defined on the basis of the animal's ability to right itself, and of alterations in the state of consciousness as indicated by ECoG activities (vide infra). For analyses of time-dependent changes, Transitional, Steady-State and Recovery periods were divided into 3 epochs of equal duration. These were: the beginning segment of each period (T1, S1 and R1); the middle segment of each period (T2, S2 and R2); and the end segment of each period (T3, S3 and R3). Behavioral and electrophysiological attributes associated with each period are described as follows.

Control period. A 45-min period prior to the induction of pentobarbital anesthesia. The animal was allowed to freely behave within the confines of the Faraday chamber.

Transitional period (Epochs: T1, T2, T3). The period between the time of pentobarbital administration and the time when the animal completely lost its ability to right itself. The ECoG activities at this time typically began to show a pattern of increasing amplitude and decreasing frequency.

Steady-State period (Epochs: S1, S2, S3). The period beginning 5 min after a complete loss of righting reflex, and ending when the animal demonstrated an attempt to right. The ECoG activity pattern was predominantly of the low frequency and high amplitude waveform varieties.

Recovery period (Epochs: R1, R2, R3). A two-hour period which began at the moment the animal demonstrated an attempt to right. The ECoG activities during this period typically showed a unique oscillatory pattern which was represented spectrographically by a 20–50 Hz power spectral complex.

Electrophysiological recordings of ECoG, RRU and DEMG activities were made continuously throughout the control and Transitional periods, and for the first 1 h of the Steady-State period. Intermittent recordings (10 min duration, once every 0.5 h) started 1 h after the beginning of Steady-State period. Continuous recording was resumed at the beginning of the Recovery period for 2 h.

Chemosensitivity tests. To evaluate the effect of pentobarbital on the integrity of CO_2 chemosensitivity, alveolar CO_2 loading was performed prior to the start of the control period, and 1.5 h after the beginning of the Steady-State period. Respiratory system responses to alveolar CO_2 during each test period were induced by either a 2% or a 5% air-CO_2 mixture. Gas mixtures were generated with a "gas blender" (Matheson, Multiple Dyna-Blender, Model 8219) and delivered to the recording chamber (volume≈36 l) at a rate of 50 l/min. The concentration of air (O_2, N_2) and CO_2 in the chamber during each ramp step change was continuously measured with a mass spectrometer (Model 1100 Medical Gas Analyzer; Perkin Elmer). The air or a preexisting gas mixture in the chamber could be displaced in approximately 3 min (3.2 ± 0.3 min) as indicated by the mass spectrometer. Sufficient time (4–6 min) was allowed for the air-CO_2 mixture in the recording chamber to equilibrate during each step change. Respiratory system responses were measured only when the CO_2 in the chamber had reached a steady preset level, that is, either 2% or 5%. Data representative of recovery from CO_2-induced respiratory stimulation were obtained 15 min after the CO_2-air mixture in the recording chamber had been completely replaced with air as indicated by the gas analyzer.

Data Analysis

Analog-to-digital conversions and analyses of electrophysiological data were accomplished with a Micro-VAX II Computer (Digital Equipment Corporation). Analog-to-digital conversion of RRU, DEMG and ECoG activities were performed at 10 kHz, 5 kHz and 625 Hz, respectively.

Unit data management scheme. Control RRU data were processed according to the following scheme. The temporal attributes of RRU burst duration and spike frequency of BOT and NpA neurons during awake, behaving (control) states showed complex variations with discrete changes in ongoing behavioral repertories [e.g., sniffing, deglutition, and postural modification; see (9)]. Aside from episodic state- and behavior-dependent variations in respiratory activity profile, the guinea pig generally assumed a motionless, resting posture, during which time, the periodicity of bulbar respiratory activity profile showed little, if any, temporal and phase (RRU-DEMG) irregularities. In view of the complexity of "wakefulness" respiratory activity profile, and of considerations that respiratory-related activities from the resting states are more manageable from the standpoint of statistical analysis, only those data from the resting states were used as representative control data. Descriptions of discrete state- and behavior-dependent RRU activities are beyond the scope and intent of this report and they will be the subject of future communications.

RRU signals were amplitude discriminated (Model 121 Window Discriminator; World Precision Instruments) prior to digitization. RRU data were analyzed according to the following scheme. To characterize pentobarbital-induced changes in the temporal attributes of RRU activities, the unit data were analyzed on the basis of cycle duration, burst duration, within-burst spike frequency and interspike interval analysis. Unit activity dwell time analysis was also performed to assess the extent to which pentobarbital altered the timing mechanisms unique to the RRU under investigation. Quantitatively, the unit activity dwell time is defined as the ratio of unit burst duration (T_{Burst}) to the total cycle duration (T_{Cycle}). On-line cycle-triggered histograms were used to continuously monitor the RRU-DEMG phase relationship.

Power spectral analyses of DEMG and ECoG activities. Time-averaged integration and power spectral analyses (12) were used to evaluate the extent of changes in DEMG and ECoG activities. DEMG data were sampled at a rate of 5 kHz for 32.768 s (20 epochs; 8192 points/epoch). ECoG data were sampled at a rate of 625 Hz for 32.768 s (20 epochs; 1024 points/epoch). No windows were used in this protocol. "Zero Mean" was applied to both DEMG and ECoG data. The running sums of DEMG data were "cosine-tapered" before Fast Fourier Transforms were computed ("Labstar" software; Digital Equipment Corporation). Spectra were not normalized since the sample durations were equal across control, Transitional, Steady-State and Recovery periods. DEMG spectra were smoothed with a 15-point polynomial filter prior to being plotted with a Hewlett-Packard (Model 7470A) digital plotter.

The generation of line graphs and histograms was accomplished with "Sigmaplot" (Version 3.10; Jandel Scientific).

Histology

Upon completion of experimentation, guinea pigs were anesthetized with overdoses of pentobarbital (75 mg/kg; IP). After anodal current lesions (30 μA; 30 s) were made at recording sites, animals were perfused transcardially with saline followed by a fixative which consisted of a mixture of 1% formaldehyde and 1% glutaraldehyde in 10% sucrose and 0.1 M phosphate buffer solution. The excised brainstems were stored in the fixative for at least 48 h prior to further processing. For histological verification of RRU recording sites, brainstem tissues were frozen, serially sectioned at 60 μm intervals, mounted on slides, stained with cresyl violet, and examined under a projection microscope.

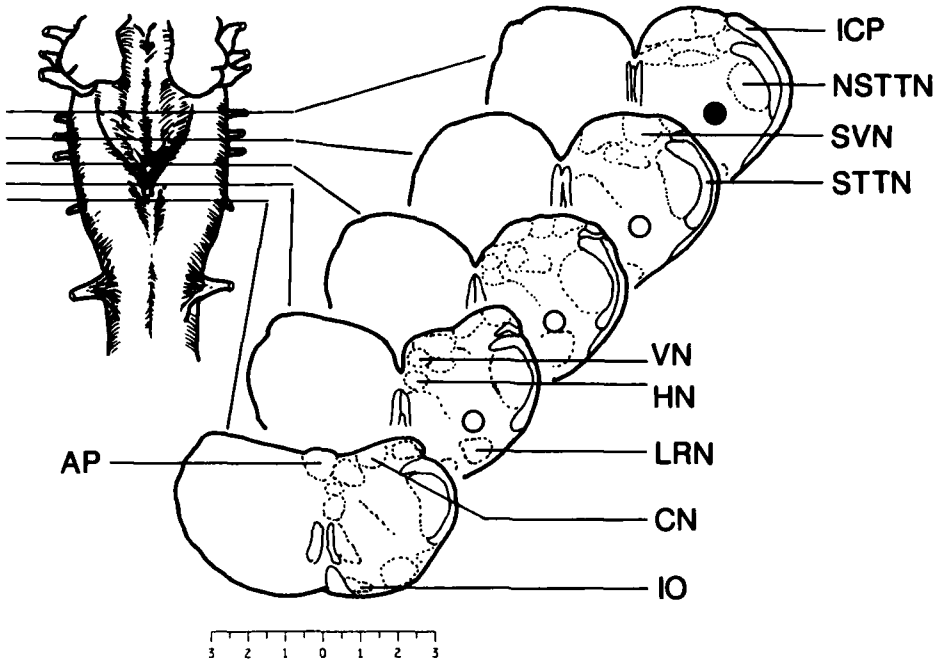

FIG. 1. A diagrammatic summary showing bulbar areas where expiratory (BOT; filled circle) and inspiratory (NpA; open circles) RRUs were recorded. Abbreviations: AP, area postrema; CN, cuneate nucleus; HN, hypoglossal nucleus; ICP, inferior cerebellar peduncle; IO, inferior olive; LRN, lateral reticular nucleus; NSTTN, nucleus spinal tract of the trigeminal nerve; STTN, spinal tract of the trigeminal nerve; SVN, spinal vestibular nucleus; VN, vagus nucleus. Calibration scale is in mm.

RESULTS

Histology

A total of 19 medullary RRUs were surveyed in this study (i.e., one unit from each animal). Ten (10) of these units were recorded from BOT (expiratory units) and the remaining nine (9) from NpA (inspiratory units). Figure 1 is a diagrammatic summary of medullary areas where recordings of BOT and NpA RRU activities were made.

Pentobarbital-Induced Bradypnea

Figure 2 is an electrophysiographic depiction of pentobarbital-induced changes in ECoG, RRU and DEMG activities across control, Transitional (duration = 3.5 ± 1.6 min), Steady-State (duration = 8.6 ± 2.1 h), and Recovery (a fixed duration of 2 h) periods. The bradypneic activity pattern of a BOT expiratory neuron is shown in Fig. 2A and the response of an NpA neuron is illustrated in Fig. 2B. The most notable change following pentobarbital was the development of a state of progressive bradypnea which began during the Transitional period (T2; 2.7 ± 1.7 min postpentobarbital). The bradypneic profile continued to progress, although at a much slower rate than that of Transitional period, during the Steady-State period to eventually reach a plateau in approximately 2 h (1.8 ± 0.5 h into the Steady-State). Henceforth, the respiratory frequency typically remained stable for about 3 h (3.4 ± 0.7 h; Steady-State). Trends toward an increase in respiratory frequency typically began during the latter half of S3 epoch. During the initial phase of the Recovery period (R1; 0–40 min into the Recovery), animals were still under the residual effects of pentobarbital and the bradypneic activity often reappeared, albeit with lesser severity, as they assumed a prone, prorated position.

Temporal Attributes of BOT and NpA Unit Responses

The development and progression of pentobarbital-induced bradypnea were accompanied by a variety of complex changes in bulbar RRU activities. Figure 3 is an epoch-to-epoch summary of changes in the temporal attributes of BOT and NpA unit activities throughout the course of anesthesia. Unit activity categories used to characterize alterations in RRU activities were the average values of cycle duration (upper left panel; Fig. 3), burst duration (upper right panel; Fig. 3), T_{Burst}/T_{Cycle} ratio (RRU activity dwell time analysis; lower left panel; Fig. 3), and RRU spike frequency (lower right panel; Fig. 3). A feature of particular interest in Fig. 3 is the considerable degree of variability (as signified by the rather large error bars) associated with each unit activity category during Transitional (T1) and Recovery (R1–R2) periods. Upon closer scrutinies of audio-visual and electrophysiographic records, this phenomenon was found to be closely related to a variety of discrete behavioral correlates. Among which, the most conspicuous were i) irregularities in chest movements; ii) a gradual loss of eyelid reflex; iii) involuntary and purposeless muscular movements; iv) uneventful postural modifications; v) diminishing responsiveness to somatosensory stimulation; and, vi) occasional vocalization. The significance of this phenomenon as it relates to the changes in respiratory functional dynamics will be described in the Discussion section of this report.

Changes in cycle and burst durations. The cycle and burst durations of BOT and NpA units showed an essentially parallel time-dependent change (increase-and-decrease) in response to

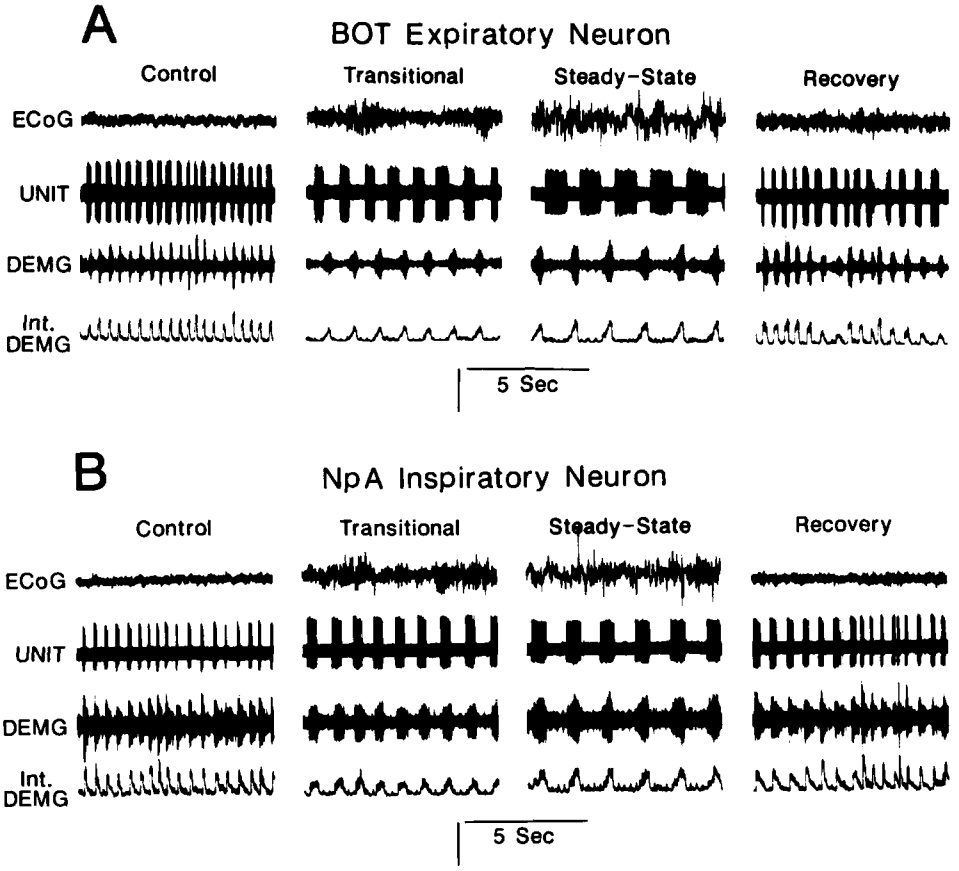

FIG. 2. (A and B) Representative electrophysiograms of ECoG, RRU and DEMG activities across control (wakefulness), Transitional (T2 at 2.32 min postpentobarbital), Steady-State (S2 at 4.07 h postpentobarbital), and Recovery (R2 at 1.00 h after the first attempt to right) periods. (A) The activity profile of a BOT expiratory unit. (B) The response pattern of an NpA inspiratory nueron. Signal trace description: ECoG, electrocorticogram; Unit, respiratory-related unit activity (A, BOT); DEMG, diaphragmatic electromyogram; Int. DEMG, integrated diaphragmatic electromyogram ($\tau = 20$ ms). Voltage calibrations: ECoG, 290 μV; UNIT, 295 μV; DEMG, 1.12 mV. The EKG artifacts in B might have been caused by a slightly nicked insulation of DEMG electrodes which occurred on occasions during recovery from surgery.

pentobarbital. An increase in cycle and burst durations typically began during the T2 epoch. A trend of reversion to a pattern comparable to that of control was usually not seen until the later part of S3 epoch. As would be expected, the time course, the direction, and the magnitude of change in BOT and NpA cycle durations were remarkably similar. A notable exception was the time-dependent change in RRU burst durations. That is, from T3 to S3 epoch, the magnitude of increase was significantly greater for BOT than NpA units. The difference between BOT and NpA burst durations was further evaluated with the T_{Burst}/T_{Cycle} ratio analysis. This technique was employed to assess the extent to which the RRU timing mechanisms were altered by pentobarbital. The analysis revealed that, while the average cycle and burst durations of BOT and NpA units both showed a notable change (increase-and-decrease), the T_{Burst}/T_{Cycle} ratios indicated that the relative BOT burst duration with reference to the cycle time was elevated to a significantly greater extent than that of NpA units. What can be inferred from this phenomenon is twofold. First, the disparity in T_{Burst}/T_{Cycle} ratios suggested that BOT and NpA neurons are differentially sensitive to the effect of pentobarbital. Second, from the standpoint of rhythmogenesis, this phenomenon indicates a profound alteration in the medullary neural network and synaptic mechanisms that are involved in the regulation of the respiratory rhythm.

RRU spike frequency. Pentobarbital-induced change in BOT and NpA spike frequencies are illustrated in the lower panel of Fig. 3. Because of the considerable variability (vide supra) seen during Transitional and Recovery periods, precisely how the direction and the magnitude of RRU spike frequencies changed during these time frames could not be clearly ascertained. Nevertheless, an unequivocal elevation in BOT and NpA spike frequencies was consistently observed throughout the course of the Steady-State. Another intriguing phenomenon seen during the Steady-State was the recurrence of high frequency spike "clusters" which appeared primarily at the beginning, and occasionally toward the end, of every burst. These "clusters" were typically made up of 2 to 3 spikes ("doublets" and "triplets"). The interspike intervals of spikes within these "clusters" were in the range of 1–2 ms. The origin and the functional significance of this phenomenon are unknown.

Pattern of within-burst spike frequency modulation. The discharge pattern of BOT units (n = 10) described in this report was

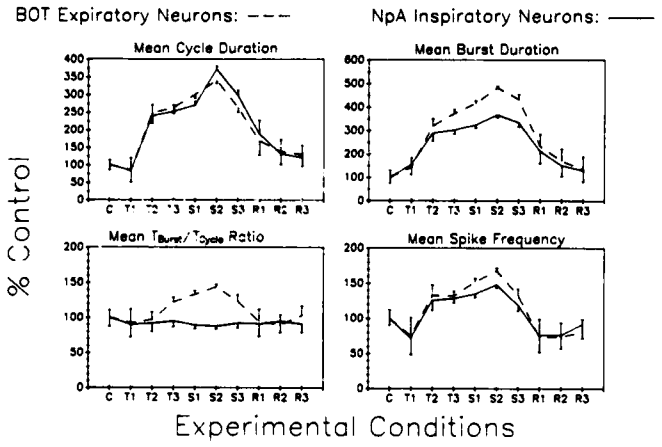

FIG. 3. An epoch-to-epoch summary of the effects of pentobarbital on RRU cycle duration, burst duration, T_{Burst}/T_{Cycle} ratio, and spike frequency. Each epoch data point represents the average response magnitude of a specific activity category across all the BOT (n = 10; dash line) units or all the NpA (n = 9; solid line) cells. Since the duration of Transitional periods were typically short-lasting (3.5 ± 1.6 min; n = 19), the data points representing T1, T2 and T3 were only of 40 s duration. Sample durations of remaining epoch data points (control, S1–S3, and R1–R3) were all of 2 min duration. For the ease of comparison, each activity category was normalized and expressed as percent of control (wakefulness). Error bars = SEM (standard error of the mean).

of the expiratory-incrementing type. With the exception of one (n = 1) tonically bursting inspiratory unit, all other NpA units (n = 8) showed a decrementing pattern. Electrophysiographic records indicated that the overall discharge character unique to each RRU was not modified appreciably by pentobarbital. Interspike interval (ISI) analyses revealed, however, some discrete changes that were not readily apparent in electrophysiographic records. Figure 4 is a summary of pentobarbital-induced changes in the ISI distribution of a representative BOT (Fig. 4A) and an NpA (Fig. 4B) units. For the BOT unit, the increase in spike frequency was represented in the ISI histograms as an increase in the number of spike events per bin. Otherwise, the profile of ISI distribution remained essentially unimodal, and the central tendency of ISI distribution was unaltered. Changes in the NpA unit were more complex. The most noticeable transformation in NpA histograms was the reorganization of a unimodal ISI distribution to that of a dispersed, multimodal profile during the Steady-State. Also noteworthy during this period was a shift of the central tendency of ISI distribution from 14-ms bin to 9-ms bin. These findings indicated once again that BOT and NpA units were affected differentially during pentobarbital anesthesia.

Diaphragmatic Responses

The extent of change in diaphragmatic activity pattern during pentobarbital anesthesia was considerable. Figure 5A is a representative spectrographic depiction of variations in DEMG power spectra throughout the course of pentobarbital anesthesia. In addition to a marked decline in DEMG amplitudes, the temporal attributes of the integrated DEMG during Transitional and Steady-State periods also underwent transformation from a brisk rise-and-fall shape to a slow-to-rise profile (see Int. DEMG traces, Fig. 2A and B), indicating therefore, a diminished extent of diaphragmatic neuromuscular interaction.

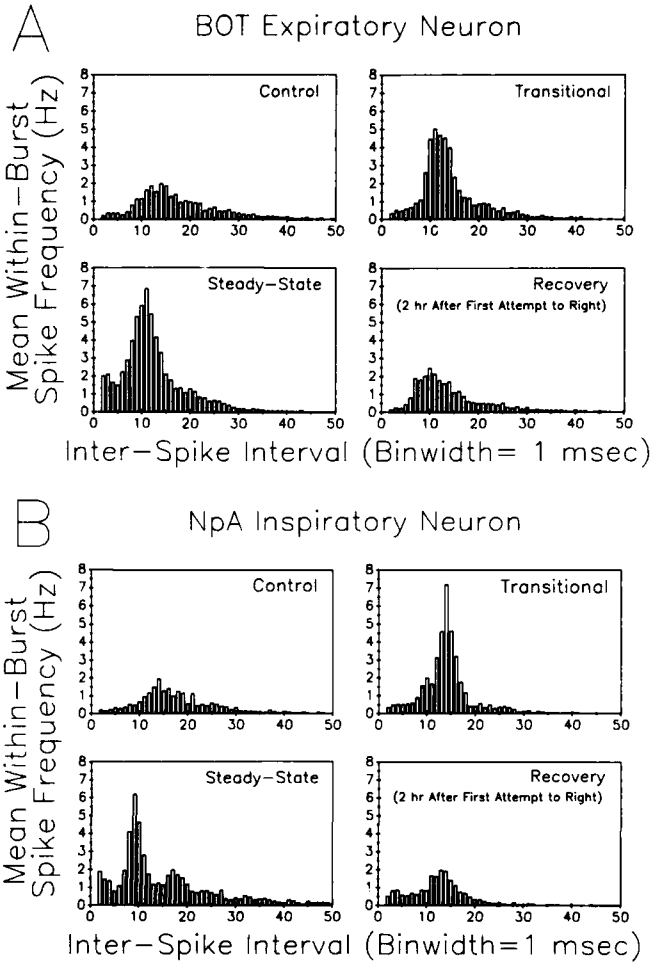

FIG. 4. (A and B) Interspike interval (ISI) analysis of pentobarbital-induced alterations in within-burst spike frequency modulation pattern of a representative BOT (A) and an NpA (B) units. Each histogram was based on data from 40 bursts taken from i) control condition, ii) T2 epoch, iii) S2 epoch; and, iv) 2 h after the animal made a first attempt to right. To permit direct comparison across experimental conditions, the ordinates had been normalized and expressed as numbers of spike events per burst per second.

ECoG Responses

Representative changes in ECoG activity patterns before, during, and after pentobarbital anesthesia are illustrated by power spectrographs in Fig. 5B. Alterations in ECoG typically took place before the animal had completely lost its ability to maintain a righted posture (T2; 2.9 ± 0.7 min postpentobarbital). The first noticeable changes in the ECoG spectral composition were i) an increasing amplitude; ii) a mixture of high and low frequency spectral varieties; and, iii) a recurrence of intermittent volleys of "sleep spindle-like" complexes. This pattern generally lasted about 30 s to 1 min which then abruptly transformed into an activity profile consisting primarily of low frequency and high amplitude spectral varieties. A low frequency, high amplitude ECoG pattern generally began during the T3 epoch and remained fundamentally unchanged throughout the Steady-State period. During the 2-h Recovery period, the ECoG activity pattern typically

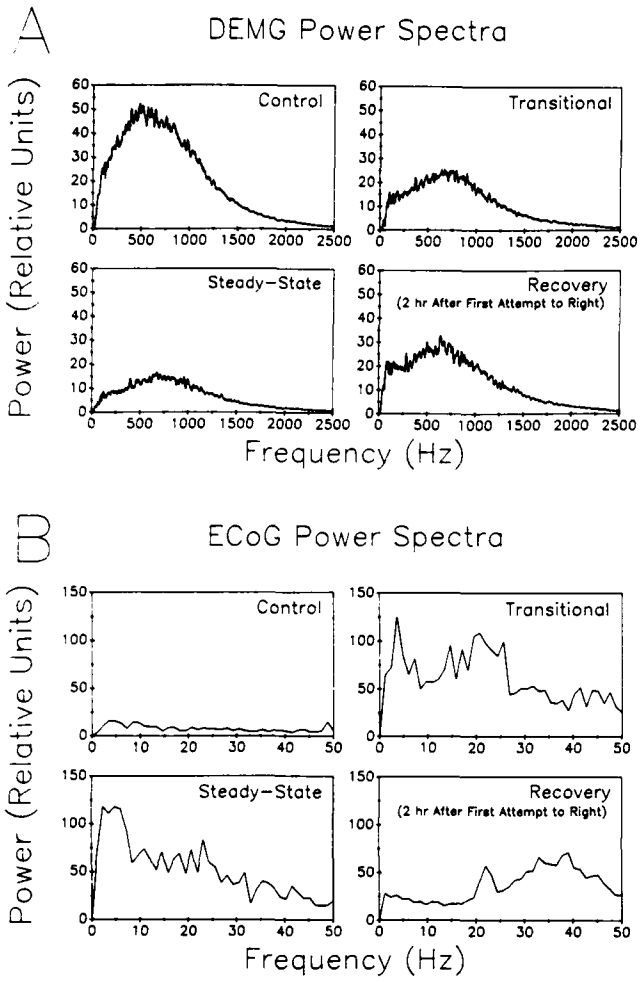

FIG. 5. (A and B) Representative time-averaged integration and spectral analysis of diaphragmatic EMG (DEMG; A) and electrocorticographic (ECoG; B) across control, Transitional (T2), Steady-State (S2) and Recovery (2 h after first attempt to right) periods. (A) The overall distribution profile of DEMG spectral components were not altered considerably by pentobarbital. The magnitude of DEMG power, however, was greatly reduced throughout the course of anesthesia, as well as during the Recovery period. (B) The most notable change in the ECoG activity was the transformation from a wakefulness ECoG pattern (low amplitude, high frequency) to a highly synchronous (low frequency, high amplitude) profile during Transitional and Steady-State periods. The ECoG activity pattern during the Recovery period typically showed a unique oscillatory pattern which was spectrographically represented by a 20–50 Hz complex.

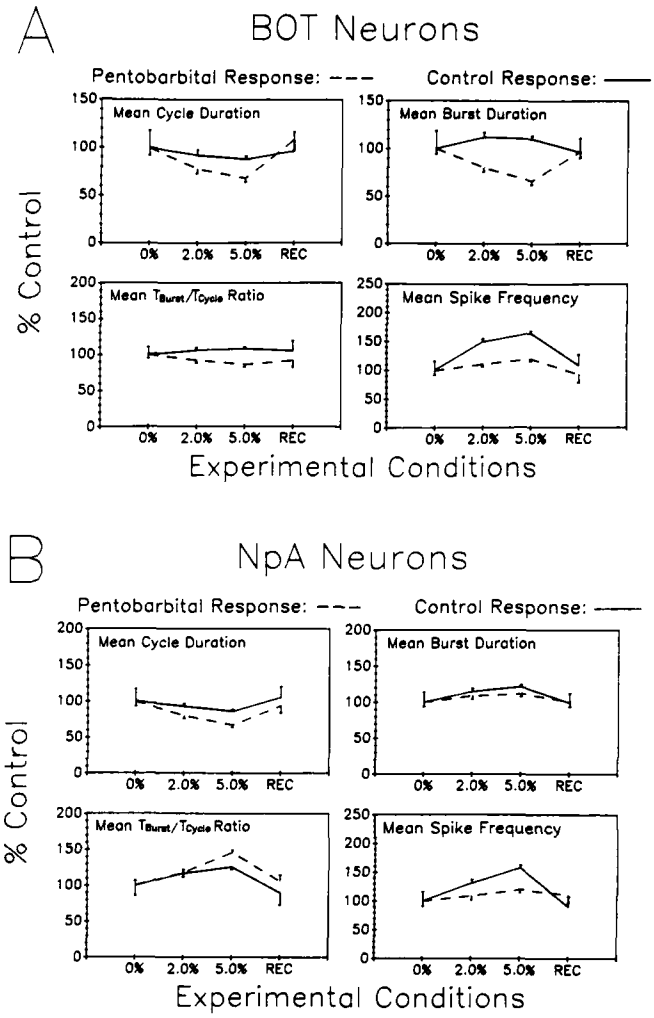

FIG. 6. (A and B) Changes in temporal attributes of BOT (A) and NpA (B) unit activities in response to alveolar CO_2 (2% and 5%) loading during control (solid line) and anesthesia (dash line) states. Each data point represents the average (BOT, n = 10; NpA, n = 9) of a 90-s sample duration. Abbreviations: 0%—room air; REC—recovery from alveolar CO_2 loading.

showed a unique oscillatory pattern which was spectrographically represented by a 20–50 Hz complex. In experiments (n = 6) where observations were continued beyond the 2-h Recovery period, it was found that from the time of first attempt to right, a duration of approximately 4 h (4.4 ± 0.7 h) was required for the ECoG to undergo a complete return to a control spectral profile.

Responses to Alveolar CO_2 Loading

Figure 6 is a summary of BOT (Fig. 6A) and NpA (Fig. 6B) unit responses to 2% and 5% alveolar CO_2 loadings during control (wakefulness) and Steady-State (anesthesia) conditions.

BOT unit responses (Fig. 6A). In awake, behaving states, 2% and 5% alveolar CO_2 loadings produced a discernible but statistically insignificant decrease in the mean cycle duration (upper left panel of Fig. 6A). The mean BOT burst duration (upper right panel of Fig. 6A), on the other hand, showed a slight increase in response to CO_2. Again, the magnitude of change was not significant. It should be mentioned that, despite an insignificant statistical outcome, the direction of change in cycle (decrease) and burst (increase) durations mentioned above was a consistently and repeatedly observable phenomenon across animals. Results of T_{Burst}/T_{Cycle} analysis (lower left panel of Fig. 6) showed that despite clear indication of an opposite response direction between cycle and burst durations, change in BOT timing attributes during alveolar CO_2 loading was not notable. Thus, during awake, behaving states, the only statistically significant change in BOT unit discharge pattern in response to CO_2 was an increase in unit spike frequency (lower right panel of Fig. 6A). Stated otherwise, in the

absence of pentobarbital, the BOT unit responses to hypercapnic challenge appears to involve primarily an increase in the spike frequency. Other activity attributes such as cycle and burst durations, which describe the timing or the temporal attributes of BOT activities, were essentially unmodified.

In the presence of pentobarbital (Steady-State), although the spike frequency of BOT units also showed a slight increase in response to CO_2, the magnitude of such an increase, however, pales in comparison to the increase seen during control states. More striking, however, were the changes in BOT cycle and burst durations. In contrast to a modest degree of change during control states, the average values of cycle and burst durations both displayed a statistically significant decrease in response to 2% and 5% CO_2. The change in burst duration is particularly noteworthy in that the response was clearly moving in a direction diametrically opposed to that of the control state. Notwithstanding a somewhat parallel decrease in cycle and burst durations, only 5% CO_2 was able to induce a significant decrease in the T_{Burst}/T_{Cycle} ratio. Thus, in the presence of pentobarbital, the BOT response to CO_2 loading does not seem to encompass an increase in spike frequency as in awake states. Instead, the hypercapnic response profile appears to involve primarily an increase in cycle frequency (or a decrease in cycle duration), and a decrease in burst duration.

Taken together, these findings suggest a profound pentobarbital-induced alteration in the functional dynamics and the timing attributes of BOT neurons. Moreover, the greatly diminished magnitude of spike frequency in response to CO_2 during Steady-States indicates either an altered state of neuronal excitability (direct effects on BOT, ventral medullary CO_2 receptors, or other sites), or an extensively modified synaptic interaction between BOT neurons and ventral medullary chemoreceptors (indirect effects). Finally, equally suggestive of a fundamental alteration in the medullary respiratory network dynamics was the asymmetric change in the BOT burst duration between control and anesthesia states.

NpA unit responses (Fig. 6B). Under control conditions, the mean cycle duration (upper left panel of Fig. 6B) of NpA units typically showed an insignificant decrease to 2% and 5% CO_2. The mean burst duration (upper right panel of Fig. 6B), on the other hand, increased in response to CO_2 although the magnitude of such a change was significant only in the presence of 5% CO_2. T_{Burst}/T_{Cycle} ratio analysis (lower left panel of Fig. 6B) revealed a significant increase across 2% and 5% CO_2, which is consistent with the direction and magnitude of changes in cycle (decrease) and burst (increase) durations. Like BOT neurons, NpA spike frequency also showed a significant increase in response to 2% and 5% CO_2. Thus, during wakefulness states, the NpA response to hypercapnic challenge appears to involve primarily an augmentation in the spike frequency, and secondarily, an increase in burst duration.

Under pentobarbital anesthesia, changes in NpA activity categories in response to CO_2 followed essentially the same direction as those of wakefulness states. In terms of response magnitudes, the NpA cycle duration was significantly decreased during 2% and 5% alveolar CO_2 loadings. The burst duration, however, showed a slight but insignificant increase. In agreement with the direction and magnitude of change in cycle and burst durations, T_{Burst}/T_{Cycle} ratio analysis revealed an almost linear increase. Thus, under anesthesia states, the NpA response to hypercapnic crisis seems to include primarily an increase in respiratory cycle frequency (i.e., a decrease in cycle duration), and to a lesser extent, an increase in burst duration and spike frequency.

During wakefulness states, the direction and the magnitude of change in NpA cycle duration, burst duration, and spike frequency in response to CO_2 were rather similar to those of BOT units. Under pentobarbital anesthesia, only the cycle duration and spike frequency of BOT and NpA units appeared to share a similar response direction. The response directions of BOT and NpA burst durations, however, seemed to move in an opposite fashion during hypercapnic challenge. That is, instead of a marked decrease seen in BOT units (Steady-State response curve; upper right panel of Fig. 6A), the burst duration of NpA units displayed a discernible, albeit statistically insignificant, increase in response to CO_2. These findings indicate that the neuronal behavior, and other aspects of the functional dynamics as well, of BOT and NpA neurons are not equally modified by pentobarbital.

DISCUSSION

This study offers direct evidence from physiologically and structurally intact preparations that a variety of physiological and functional attributes of bulbar respiratory-related neurons are profoundly altered by sodium pentobarbital. Although it is not the intent of this study to provide a definitive account of the underlying mechanisms involved in pentobarbital-induced respiratory depression, findings derived from this study uncover a host of discrete changes that can be used as a conceptual framework and reference database with which more systematic investigations may be designed and executed. The significance of these changes as they relate to the functional dynamics of bulbar rhythmogenic mechanisms will be addressed.

The most notable alteration in the respiratory pattern following the induction of pentobarbital anesthesia was a progressive reduction in the respiratory frequency (Fig. 3). Electrophysiographically, these events appear to be related to the increase in the cycle duration of both BOT and NpA neurons. In addition, it was shown that while the burst durations of BOT and NpA units both displayed an increase under pentobarbital, the relative increase in burst duration was significantly greater for BOT than NpA units as revealed by T_{Burst}/T_{Cycle} ratio analysis. The differential responsiveness of BOT and NpA units to pentobarbital was also manifested in the temporal attributes of their response patterns to alveolar CO_2 loading (Fig. 6). Taken together, these findings suggest that pentobarbital does not only exert an unequal influence on the neuronal behaviors of BOT and NpA units, but it also produces a fundamental alteration in the bulbar rhythmogenic timing mechanisms.

Pentobarbital has been shown in this study to cause a variety of changes in the behaviors of RRU spike activities. In addition to a striking alteration in the pattern of modulation of within-burst spike frequency (Fig. 4), pentobarbital was also found to cause an elevation in the spike frequencies (Figs. 3, 4) of both BOT and NpA neurons vis-à-vis an unabating depression in diaphragmatic spectral powers (Fig. 5A). The increase in RRU spike frequency is somewhat unexpected since the depressant effects of pentobarbital would be expected to cause a decrease in the RRU excitability. It is not known whether or not the increase in spike frequency represents an altered state of synaptic interaction within the bulbar rhythmogenic network. Previous investigations, however, have identified an increase in arterial CO_2 gas tension during pentobarbital anesthesia (24,28). The possibility remains, therefore, that the increase in RRU spike frequency during pentobarbital anesthesia might have been the result of an increased hypercapnic burden which culminates in a maintained stimulation on an already depressed bulbar rhythmogenic neural network.

The immoderate degree of variability in the temporal attributes of RRU activity profile (cycle duration, burst duration and RRU spike frequency) during Transitional (T1) and Recovery (R1–R2) periods is also noteworthy. Upon careful examinations of electrophysiographic records and analyses of spike data on a burst-to-burst basis, it was established that the variability was neither a

result of an unusually large difference across subjects, nor an ungainly outcome of statistical averaging. Instead, the variability appeared to represent considerable fluctuations in the activity patterns of the bulbar rhythmogenic mechanisms during the induction (Transitional period) and the recuperative (Recovery period) phases of pentobarbital anesthesia. What may be inferred from these phenomena is two-fold.

First, during Transitional periods, the rather large variability in RRU activity patterns may actually indicate a state of ongoing alteration and reorganization of the bulbar rhythmogenic mechanism as the effects of pentobarbital became increasingly pronounced. Electrophysiographically, this state can be identified by an occasional aperiodic RRU cycle rhythm, a variable burst duration, a marked reduction in the amplitude of DEMG oscillations, and a transformation of ECoG acitivity from a wakefulness pattern (low amplitude, high frequency) to that of an increasing amplitude and decreasing frequency. Clinically, this phenomenon may very well be the underlying events of life-threatening respiratory depression commonly noted during the induction phase of surgical anesthesia. The fluctuating RRU activity pattern mentioned above also poses some interesting questions from the standpoint of experimental and clinical applications of anesthetic agents. For example, for a comparable depth of steady-state anesthesia, would some anesthetics present a greater degree of disruption to the respiratory system than others during the induction phase, and thus engender a life-threatening crisis? What, and how, are the adjuncts (e.g., an short-acting respiratory stimulant) when coadministered with an anesthetic agent would offer a wider margin of safety during the induction phase? These questions should be taken into serious consideration in the design, development and use of a novel anesthetic agent.

Second, during the Recovery period, the large variance of RRU activity profile may represent a state of "conflict" within the bulbar rhythmogenic mechanisms as the emerging wakefulness influence increases while the depressant effect of pentobarbital declines.

The functional capacity of bulbar rhythmogenic neural substrates is a complex neurophysiological phenomenon [for review, see (14,15)]. Despite its seemingly rhythmic and invariant appearance, bulbar respiratory-related unit activity patterns can undergo considerable changes in response to a variety of intrinsic and extrinsic stimuli (e.g., temperature, hypoxia, hypercapnia, vago-pulmonary afferents, forebrain centrifugal influence, hormonal fluctuations, somatosensory afferents during postural modification, phonation, sleep and wakefulness cycle, etc.). Implicit within this message, and particularly in consideration of the fluctuating tissue oxygen demand on a moment-to-moment basis, it should be no less than a neurophysiological certainty that the bulbar rhythmogenic mechanism be endowed with a functionally dynamic predisposition with which to effectively cope with a variety of unpredictable and extreme physiological demands. The effects of pentobarbital on respiration described in this report may serve as a case in point: While the remarkable difference in the neuronal behaviors of RRUs between wakefulness and anesthesia states may be explained entirely on the basis of aberrant effect of pentobarbital, one cannot help but be also impressed by the functional plasticity of the bulbar rhythmogenic mechanisms, and, the extent to which the functional dynamics of bulbar respiratory system components change in response not only to the depressant effects of pentobarbital anesthesia, but also, in other states, to a multiplicity of physically and physiologically taxing circumstances.

The scientific and technical merits of the model system used in this study can be measured in two parts. First, the very foundation of respiratory neurophysiology is still based primarily on experimental data derived from anesthetized or paralyzed preparations. Little, if anything, is known about the nature and extent of the modulatory influences of wakefulness on the bulbar respiratory rhythmogenic mechanisms. The methodology used in this study, therefore, may serve to bring about a better understanding of the operational dynamics and functional plasticity of bulbar respiratory rhythmogenesis relative to various behavioral repertories and altered states of consciousness. Second, in addition to a physiologically "unnatural" respiratory status, anesthetic agents have also been shown to interact with a variety of drugs (29) to produce a mélange of untoward cardiovascular effects (24). Free of the confounding and deleterious effects of anesthetics, the present model system may be of considerable value not only as an experimental tool in the design of a more effective medical management program for acute and chronic respiratory diseases, but also in investigations of the neurophysiology and neuropharmacology of medullary respiratory rhythmogenesis.

ACKNOWLEDGEMENTS

I would like to thank Raul Olaya, Frank S. Hovatter, Leslie Metker and Delores Tucker for their excellent assistance in surgery, recording, data analysis and histology. My appreciation is also extended to Dr. F. J. Lebeda and Dr. F. J. Cann for their critical review of the manuscript. The opinions and assertions contained in this report are the personal views of the authors and are not to be construed as official or as reflecting the views of U.S. Army or the Department of Defense. In conducting the research described in this report, the investigator adhered to the "Guide for the Care and Use of Laboratory Animals of the Institute of Laboratory Animal Resources, National Research Council."

REFERENCES

1. Batsel, H. L. Activity of bulbar respiratory neurons during passive hyperventilation. Exp. Neurol. 19:357–374; 1967.
2. Bianchi, A. L.; Barillot, J. C. Effects of anesthesia on activity patterns of respiratory neurones. Adv. Exp. Med. Biol. 99:17–22; 1978.
3. Bianchi, A. L.; Barillot, J. C. Respiratory neurons in the region of the retrofacial nucleus: Pontile, medullary, spinal and vagal projections. Neurosci. Lett. 31:277–282; 1982.
4. Bouverot, P.; Crance, J. P.; Dejours, P. Factors influencing the intensity of the Breuer-Hering inspiration-inhibition reflex. Respir. Physiol. 8:376–384; 1970.
5. Brodie, D. A. The effect of thiopental and cyanide on the activity of inspiratory neurons. J. Pharmacol. Exp. Ther. 126:264–269; 1959.
6. Budzinska, K.; von Euler, C.; Kao, F. F.; Pantaleo, T.; Yamamoto, Y. Effects of graded focal cold block in the solitary and para-ambigual regions of the medulla in the cat. Acta Physiol. Scand. 124: 317–328; 1985.
7. Budzinska, K.; von Euler, C.; Kao, F. F.; Pantaleo, T.; Yamamoto, Y. Effects of graded focal cold block in rostral areas of the medulla. Acta Physiol. Scand. 124:329–340; 1985.
8. Caille, D.; Vibert, J.-F.; Bertrand, F.; Gromysz, H.; Hugelin, A. Pentobarbitone effects on respiration related units: selective depression of bulbopontine reticular neurones. Respir. Physiol. 36:201–216; 1979.
9. Chang, F.-C. T.; Foster, R. E. Medullary inspiratory-related unit discharge patterns in awake, behaving guinea pigs. Soc. Neurosci. Abst. 12:305; 1986.
10. Chang, F.-C. T.; Harper, R. M. A procedure for chronic recording of diaphragmatic electromyographic activity. Brain Res. Bull. 22: 561–563; 1989.
11. Chang, F.-C. T.; Scott, T. R.; Harper, R. M. Methods of single unit recording from medullary neural substrates in awake, behaving guinea pigs. Brain Res. Bull. 21:749–756; 1988.
12. Childers, D. G. Modern spectrum analysis. New York: IEEE Press; 1978.

13. Fedorko, L.; Merrill, E. G. Axonal projections from the rostral expiratory neurons of the Bötzinger Complex to medulla and spinal cord in the cat. J. Physiol. (Lond.). 350:487–496; 1984.
14. Feldman, J. L.; Neurophysiology of breathing in mammals. In: Bloom, F. E., ed. Handbook of physiology. The nervous system, part IV, Intrinsic regulatory systems of the brain. Bethesda: American Physiological Society; 1986:463–524.
15. Fishman, A. P.; Cherniack, N. S.; Widdicombe, J. G.; Geiger, S. R. Handbook of physiology. sect. 3: The respiratory system; vol. II. Control of breathing, parts I and II. Bethesda: American Physiological Society; 1986.
16. Flórez, J.; Borison, H. L. Effects of central depressant drugs on respiratory regulation in the decerebrate cat. Respir. Physiol. 6:318–329; 1969.
17. Gautier, H. Pattern of breathing during hypoxia or hypercapnia of the awake or anesthetized cat. Respir. Physiol. 27:193–206; 1976.
18. Harris, T. D.; Borison, H. L. Effects of pentobarbital on electrical excitability of respiratory center in the cat. Am. J. Physiol. 176:77–82; 1954.
19. Kalia, M. P. Anatomical organization of central respiratory neurons. Annu. Rev. Physiol. 43:105–120; 1981.
20. Kalia, A.; Feldman, J. L.; Cohen, M. I. Afferent projection to the inspiratory neuronal region of the ventrolateral nucleus of the tractus solitarius in the cat. Brain Res. 161:25–38; 1979.
21. Lipski, J.; Merrill, E. G. Electrophysiological demonstration of the projection from expiratory neurones in the rostral medulla to contralateral dorsal respiratory group. Brain Res. 197:521–524; 1980.
22. Otake, K.; Sasaki, H.; Mannen, H.; Ezure, K. Morphology of expiratory neurons of the Bötzinger Complex: An HRP study in the cat. J. Comp. Neurol. 258:565–579; 1987.
23. Phillipson, E. A.; Hickey, R. F.; Graf, P. D.; Nadel, J. A. The Hering-Breuer inflation reflex and regulation of breathing in conscious dogs. J. Appl. Physiol. 31:746–750; 1971.
24. Priano, L. L.; Traber, D. L.; Wilson, R. D. Barbiturate anesthesia: An abnormal physiologic situation. J. Pharmacol. Exp. Ther. 165: 126–135; 1969.
25. Richardson, P. S.; Widdicombe, J. G. The role of the vagus nerves in the ventilatory responses to hypercapnia and hypoxia in anesthetized rabbits. Respir. Physiol. 7:122–135; 1969.
26. Robson, J. G.; Housely, M. A.; Solis-Quiroga, O. H. The mechanism of respiratory arrest with sodium pentobarbital and thiopental. Ann. NY Acad. Sci. 109:494–502; 1963.
27. Seyama, I.; Narahashi, T. Mechanism of blockade of neurotransmission by pentobarbital. J. Pharmacol. Exp. Ther. 192:94–104; 1975.
28. Steiner, S. H.; Calvin, J. R. The effects of anesthesia with pentobarbital on hemodynamics and arterial blood gas in splenectomized dogs. J. Thorac. Cardiovasc. Surg. 54:592–598; 1967.
29. Trulson, M. E. Pharmacological investigation of CNS unit responses in awake, freely moving animals. Trends Pharmacol. Sci. 5:287–289; 1984.
30. Wang, S. C.; Nims, L. F. The effect of various anesthetics and decerebration on the CO_2 stimulating action on respiration in cats. J. Pharmacol. Exp. Ther. 92:187–195; 1948.